

# A novel Hsp90 inhibitor to disrupt Hsp90/Cdc37 complex against pancreatic cancer cells

Tao Zhang,<sup>1</sup> Adel Hamza,<sup>2</sup> Xianhua Cao,<sup>1</sup>  
Bing Wang,<sup>1</sup> Shuwen Yu,<sup>1</sup> Chang-Guo Zhan,<sup>2</sup>  
and Duxin Sun<sup>1</sup>

<sup>1</sup>Division of Pharmaceutics, College of Pharmacy, The Ohio State University, Columbus, Ohio and <sup>2</sup>Department of Pharmaceutical Sciences, College of Pharmacy, University of Kentucky, Lexington, Kentucky

## Abstract

Pancreatic cancer is an aggressive disease with multiple biochemical and genetic alterations. Thus, a single agent to hit one molecular target may not be sufficient to treat this disease. The purpose of this study is to identify a novel Hsp90 inhibitor to disrupt protein-protein interactions of Hsp90 and its cochaperones for down-regulating many oncogenes simultaneously against pancreatic cancer cells. Here, we reported that celastrol disrupted Hsp90-Cdc37 interaction in the superchaperone complex to exhibit antitumor activity *in vitro* and *in vivo*. Molecular docking and molecular dynamic simulations showed that celastrol blocked the critical interaction of Glu<sup>33</sup> (Hsp90) and Arg<sup>167</sup> (Cdc37). Immunoprecipitation confirmed that celastrol (10  $\mu\text{mol/L}$ ) disrupted the Hsp90-Cdc37 interaction in the pancreatic cancer cell line Panc-1. In contrast to classic Hsp90 inhibitor (geldanamycin), celastrol (0.1-100  $\mu\text{mol/L}$ ) did not interfere with ATP binding to Hsp90. However, celastrol (1-5  $\mu\text{mol/L}$ ) induced Hsp90 client protein degradation (Cdk4 and Akt) by 70% to 80% and increased Hsp70 expression by 12-fold. Celastrol induced apoptosis *in vitro* and significantly inhibited tumor growth in Panc-1 xenografts. Moreover, celastrol (3 mg/kg) effectively suppressed tumor metastasis by more than 80% in RIP1-Tag2 transgenic mouse model with pancreatic islet cell carcinogenesis. The data suggest that celastrol is a novel Hsp90 inhibitor to disrupt Hsp90-Cdc37 interaction against pancreatic cancer cells. [Mol Cancer Ther 2008;7(1):162–70]

Received 7/18/07; revised 10/23/07; accepted 11/28/07.

The costs of publication of this article were defrayed in part by the payment of page charges. This article must therefore be hereby marked *advertisement* in accordance with 18 U.S.C. Section 1734 solely to indicate this fact.

**Requests for reprints:** Duxin Sun, Division of Pharmaceutics, College of Pharmacy, The Ohio State University, 500 West 12th Avenue, Columbus, OH 43210. Phone: 614-292-4381; Fax: 614-292-7766. E-mail: sun.176@osu.edu

Copyright © 2008 American Association for Cancer Research.  
doi:10.1158/1535-7163.MCT-07-0484

## Introduction

Pancreatic cancer is the fourth leading cause of cancer death in the United States (1). The overall 5-year survival rate for pancreatic cancer patients is only 4% due to the lack of treatment options (2). Currently, targeted therapy against a malfunctioning molecule or pathway has produced promising results for various solid tumors, such as Gefitinib against lung cancer, Avastin and Ebitux against colon cancer, Herceptin against breast cancer, and SU-011248 against kidney cancer (3, 4). However, clinical trials using antibodies against epidermal growth factor receptor, vascular endothelial growth factor, and HER-2 in pancreatic cancer have had minimal benefits (5–7). Considering the complexity of pancreatic cancer with its multiple genetic abnormalities, targeting a single pathway is unlikely to be effective. Thus, identification of new targets that modulate multiple signaling pathways would be desired for treating pancreatic cancer.

Therefore, targeting molecular chaperone Hsp90 may offer many advantages for pancreatic cancer therapy due to its simultaneous regulation of various oncogenic proteins (8, 9). Most of Hsp90 client proteins (HER-2/*neu*, epidermal growth factor receptor, Akt, Cdk4, Bcr-Abl, p53, and Raf-1) are essential for cancer cell survival and proliferation (9). Chaperoning of these client proteins is regulated through a dynamic cycle driven by ATP binding to Hsp90 and subsequent hydrolysis (10). Hsp90 requires a series of cochaperones to form a complex for its function. These cochaperones, including Cdc37, Hsp70, Hsp40, Hop, Hip, p23, pp5, and immunophilins, bind and release in the superchaperone complex at various times to regulate the folding, assembly, and maturation of Hsp90 client proteins (10). A well-known mechanism of Hsp90 inhibition involves the compounds geldanamycin and its derivative 17-allylamino-geldanamycin blocking ATP binding to Hsp90. These compounds cause the catalytic cycle of Hsp90 to arrest in the ADP-bound conformation, subsequently leading to premature release and degradation of client proteins (10). This method has proven to be feasible therapeutically, such that 17-allylamino-geldanamycin has entered clinical trials (11).

However, all current Hsp90 inhibitors employ the same mechanism of ATP blockage for inactivating this chaperone. None of these inhibitors has received the Food and Drug Administration approval. It would be premature to conclude that the strategy of blocking the ATP binding to Hsp90 is a viable approach for the development of a Hsp90 inhibitor. In addition, many compounds that might have inhibited the function of Hsp90 were probably excluded during drug screening simply because they could not bind to the ATP pocket. Because the Hsp90 chaperoning process involves the transient formation of multiprotein complexes with cochaperones, halting the chaperoning cycle at

various stages is also likely to achieve Hsp90 inhibition. Thus, we hypothesize that disruption of the interaction of Hsp90 with its cochaperones will achieve Hsp90 inhibition against cancer cells.

Because one of the essential cochaperones is Cdc37, which associates client proteins to Hsp90, we intend to identify a Hsp90 inhibitor that disrupts the Hsp90-Cdc37 interaction against pancreatic cancers in the present study. We hypothesize that disruption of Hsp90-Cdc37 interaction, without affecting ATP binding to Hsp90, should have similar anticancer effects as treatment with 17-allylamino-geldanamycin and geldanamycin. Previous studies have shown that celastrol (Fig. 1A), a quinone methide triterpene from *Tripterygium wilfordii* Hook F regulated the Hsp90 pathway and induced the heat shock response similar to other Hsp90 inhibitors (12, 13). We found that celastrol did not effect ATP binding to Hsp90. Using molecular modeling, we identified that celastrol blocked Cdc37 binding to Hsp90. Indeed, immunoprecipitation confirmed that celastrol disrupted the Hsp90-Cdc37 complex. This disruption resulted in degradation of Hsp90 client proteins to induce apoptosis in pancreatic cancer cell line Panc-1 *in vitro*. In addition, celastrol exhibited anticancer activity in Panc-1 xenograft model and RIP1-Tag2 transgenic mice

of islet tumors *in vivo*. These data provide a novel strategy for Hsp90 inhibition through disruption of Hsp90-cochaperones interaction, offering the potential of isolating Hsp90 inhibitors against pancreatic cancers.

## Materials and Methods

### Drugs and Reagents

Celastrol was purchased from Cayman Chemical, proteasome inhibitor MG132 from Calbiochem, and lactacystin from Sigma-Aldrich. Geldanamycin was kindly provided by Dr. George Wang (Department of Chemistry, The Ohio State University). The following antibodies were used for immunoblotting: Akt, Hsp90 (Cell Signaling), Hsp70, Hop (StressGen), Cdk4, Cdc37, I $\kappa$ B $\alpha$ , p27, Hsp90 (Santa Cruz), actin, and p23 (Abcam). Monoclonal Hsp90 antibody H9010 and purified Hsp90 $\beta$  protein were kind gifts of Dr. David Toft (Mayo Clinic).

### Molecular Modeling

The initial coordinates of the human Hsp90 protein used in our computational studies came from the X-ray crystal structure (1US7.pdb; ref. 14) deposited in the Protein Data Bank (15). For comparison, the yeast Hsp90-p23/Sba1 X-ray structure 2CG9.pdb was also used (16). Using these

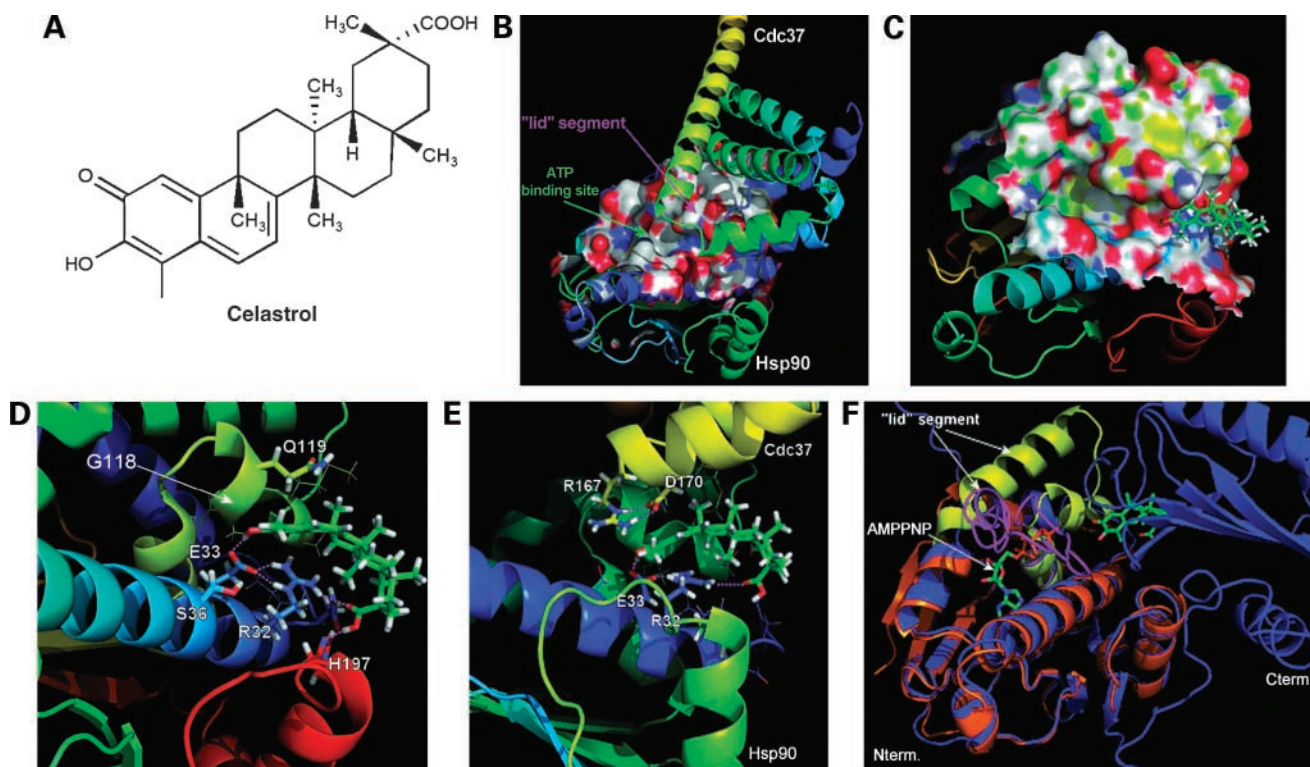


**Figure 1.** Molecular docking of celastrol with Hsp90 and Hsp90-Cdc37 complex. **A**, chemical structure of celastrol. **B**, ribbon view of the Hsp90-Cdc37 X-ray structure with the solvent accessible surface of the Hsp90-Cdc37 interface. **C**, ribbon view and solvent accessible surface of the Hsp90-celastrol binding pocket. **D**, ribbon view of the Hsp90-celastrol binding pocket. Only amino acid residues close to celastrol are displayed for clarity. **E**, ribbon view of the Hsp90-Cdc37-celastrol binding pocket. Only amino acid residues close to celastrol are displayed for clarity. **F**, ribbon view of the superimposition of Hsp90-celastrol (brown) complex with the Hsp90-p23/Sba1 (blue) X-ray structure. AMPPNP, ATP analogue; yellow, "lid" segment for HSP90-celastrol; pink, "lid" segment for Hsp90-p23. The p23/Sba1 cochaperone that is also present in the crystal has been omitted for clarity.

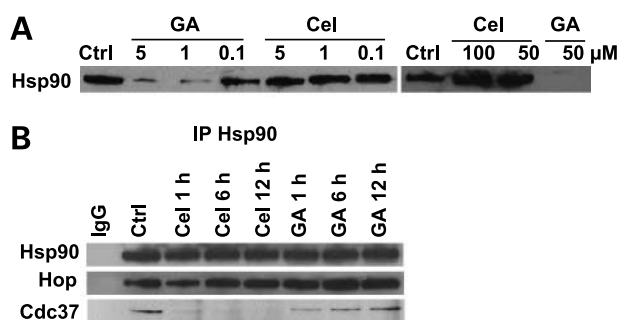


**Figure 2.** Celestrol disrupts the Hsp90-Cdc37 interaction in pancreatic cancer cells. **A**, celestrol does not inhibit ATP binding to Hsp90.  $\gamma$ -Phosphate-linked ATP-Sepharose was used to pull down Hsp90 $\beta$  in the absence or presence of geldanamycin or celestrol. Hsp90 was detected by Western blot. **B**, celestrol decreases the amount of Cdc37 proteins associated with Hsp90. Panc-1 cells were treated with 10  $\mu$ M celestrol or geldanamycin. Cell lysate was immunoprecipitated with Hsp90 antibody. Western blot was done for detection of Hsp90, Cdc37, and Hop. Cel, celestrol.

proteins, we carried out molecular docking, molecular dynamic simulations, and protein-ligand binding free energy calculations. The computational details are provided in the Supplementary Data.<sup>3</sup>

#### MTS Assay

The human Panc-1 cells were seeded in 96-well plates at a density of 3,000 to 5,000 cells per well. Twenty-four hours later, the cells were treated with increasing concentrations of either celestrol or geldanamycin as indicated. The viable cells were assessed by MTS assay after 24 h. The IC<sub>50</sub>s for cytotoxicity were calculated with WinNonlin software (Pharsight).

#### Annexin V-Enhanced Green Fluorescent Protein Assay

Control cells and cells treated with 5  $\mu$ M celestrol for various durations were stained with Annexin V-enhanced green fluorescent protein for analysis of phosphoserine inversion. The Annexin V-enhanced green fluorescent protein Apoptosis Detection Kit was obtained from BioVision Research Products. The staining was done according to the manual from manufacturer.

#### ATP-Sepharose Binding Assay

The assay was described previously (17). Briefly, 5  $\mu$ g human Hsp90 $\beta$  protein was preincubated on ice in 200  $\mu$ L incubation buffer [10 mmol/L Tris-HCl, 50 mmol/L KCl, 5 mmol/L MgCl<sub>2</sub>, 2 mmol/L DTT, 20 mmol/L Na<sub>2</sub>MoO<sub>4</sub>, 0.01% NP40 (pH 7.5)] containing celestrol or geldanamycin. Following incubation, 25  $\mu$ L pre-equilibrated  $\gamma$ -phosphate-linked ATP-Sepharose (Jena Bioscience GmbH) was added and incubated at 37°C for 30 min with frequent agitation. Sepharose was subsequently washed and analyzed by SDS-PAGE.

#### Western Blotting and Immunoprecipitation

The procedure for the Western blot analysis was briefly described as follows. After drug treatment, cells were washed twice with ice-cold PBS, collected in lysis buffer [20 mmol/L Tris (pH 7.5), 1% NP40, 150 mmol/L NaCl, 5 mmol/L EDTA, 1 mmol/L Na<sub>3</sub>VO<sub>4</sub>] supplemented with a protease inhibitor mixture (Sigma; added at a 1:100 dilution), and incubated on ice for 20 min. The lysate was then centrifuged at 14,000  $\times$  g for 10 min. Equal amounts of total protein were subjected to SDS-PAGE, transferred onto nitrocellulose membranes, and probed with appropriate antibodies. Immunoprecipitation was done as described previously (13).

#### Xenograft Mouse Model

Four- to six-week-old *nu/nu* athymic female mice were obtained from Charles River Laboratories. The human Panc-1 cells ( $5 \times 10^6$ - $10 \times 10^6$ ) were mixed with reconstituted basement membrane (Collaborative Research) and implanted s.c. to the right and left flanks of the mice. Tumor volumes were calculated with the formula: width<sup>2</sup>  $\times$  length / 2. When tumors reached 100 mm<sup>3</sup>, animals were randomized into different groups for treatment ( $n = 6$  per group).

Celestrol and geldanamycin were dissolved in the vehicle [10% DMSO, 70% Cremophor/ethanol (3:1), and 20% PBS (18)] and administered at 3 mg/kg by i.p. injection for 2 continuous days. Then, the dosing schedule was changed to one injection per 3 days. Tumor sizes and body weights were measured twice a week.

#### RIP1-Tag2 Transgenic Mouse Model

RIP1-Tag2 transgenic mice express the insulin promoter-driven SV40 T antigen and produce spontaneous multifocal and multistage pancreatic islet carcinomas. RIP1-Tag2-positive mice were identified by PCR analysis of genomic DNA from tail biopsy. RIP1-Tag2 mice (8 weeks old) were randomly divided into three groups and injected with vehicle, 3 mg/kg celestrol, or geldanamycin once every 3 days. After 4 weeks of injection, mice of each group were sacrificed and tumor tissues were collected. The remaining mice were monitored to calculate the survival rate.

## Results

### Molecular Docking of Celestrol for the Interactions with the Hsp90 Protein

To investigate whether celestrol disrupts the Hsp90-Cdc37 interaction, we first tested whether celestrol could bind Hsp90 residues located at the interface of the Hsp90-Cdc37 complex or the ATP-binding pocket of Hsp90 (Fig. 1B). *In silico* molecular modeling was used to reveal how celestrol could bind to Hsp90 and predict the corresponding Hsp90-ligand binding energy.

To explore the best possible mode of the ligand binding with Hsp90, we first did molecular docking. Then, simulated annealing and molecular dynamic simulations were carried out on a variety of possible protein-ligand binding structures. The simulated protein-ligand binding structures were used for binding free energy calculations.

<sup>3</sup> Supplementary material for this article is available at Molecular Cancer Therapeutics Online (<http://mct.aacrjournals.org/>).

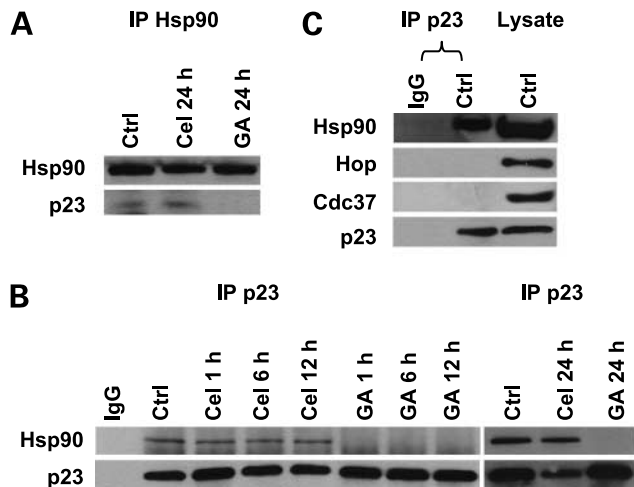


**Figure 3.** Celastrol does not disrupt Hsp90-p23 complex as geldanamycin does. **A**, Panc-1 cells treated with 10  $\mu\text{mol/L}$  celastrol or geldanamycin. The cell lysate was immunoprecipitated with Hsp90 antibody and analyzed for p23. **B**, Panc-1 cells were treated with 10  $\mu\text{mol/L}$  celastrol or geldanamycin. Cell lysate was immunoprecipitated with p23 antibody, and Western blot was done for detection of Hsp90. **C**, cochaperone p23 does not coexist with Hop or Cdc37. Panc-1 cell lysates were immunoprecipitated by p23 for detection of Hsp90, Hop, and Cdc37.

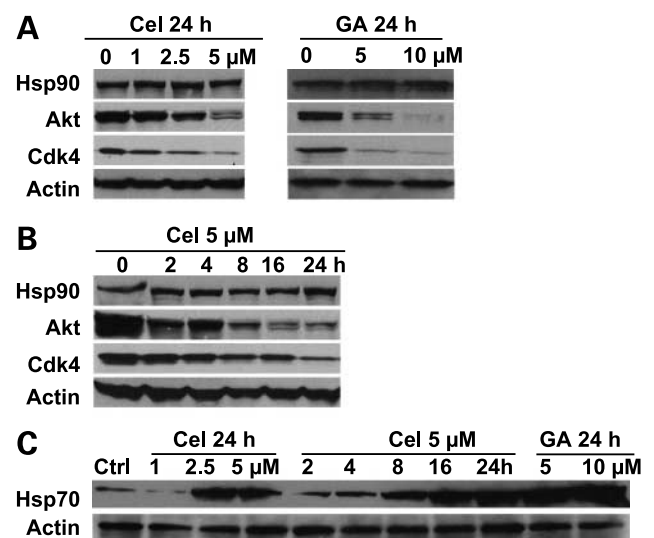
The most favorable structure of the ligand binding with Hsp90 had a binding energy of  $-18.8$  kcal/mol, excluding the entropic contribution (19). The *in silico* model of the Hsp90-celastrol binding and the subsequent molecular dynamic simulation showed that celastrol formed a favorable complex with Hsp90 in a binding site distinct from the ATP-binding pocket (Fig. 1C). Molecular dynamic trajectory of the optimum docking model revealed that the distances between celastrol and the key residues in the Hsp90-binding site were found to be stable after the first 0.5 ns of the molecular dynamic simulation (Supplementary Fig. S7B).<sup>3</sup> The cyclohexadienone moiety of celastrol was bound to a polar groove of Hsp90 that was defined by several residues in the lid segment (residues 94-125) and the mouth of the nucleotide-binding pocket. Thus, the hydroxyl and carbonyl groups of celastrol protruded into a polar and charged pocket, which was surrounded by the side chains Gln<sup>119</sup>, Glu<sup>33</sup>, Arg<sup>32</sup>, and Gly<sup>118</sup> (Fig. 1D; Supplementary Fig. S7A).<sup>3</sup> In addition, these groups occupied the positions suitable for the formation of a H-bond between Glu<sup>33</sup> and the NH group of the Gly<sup>118</sup> backbone, whereas the carboxyl moiety of celastrol formed two other H-bonds with the side chains of Arg<sup>32</sup> and His<sup>197</sup>.

#### Molecular Modeling of the Possible Binding between the Hsp90-Celastrol Complex and Cdc37

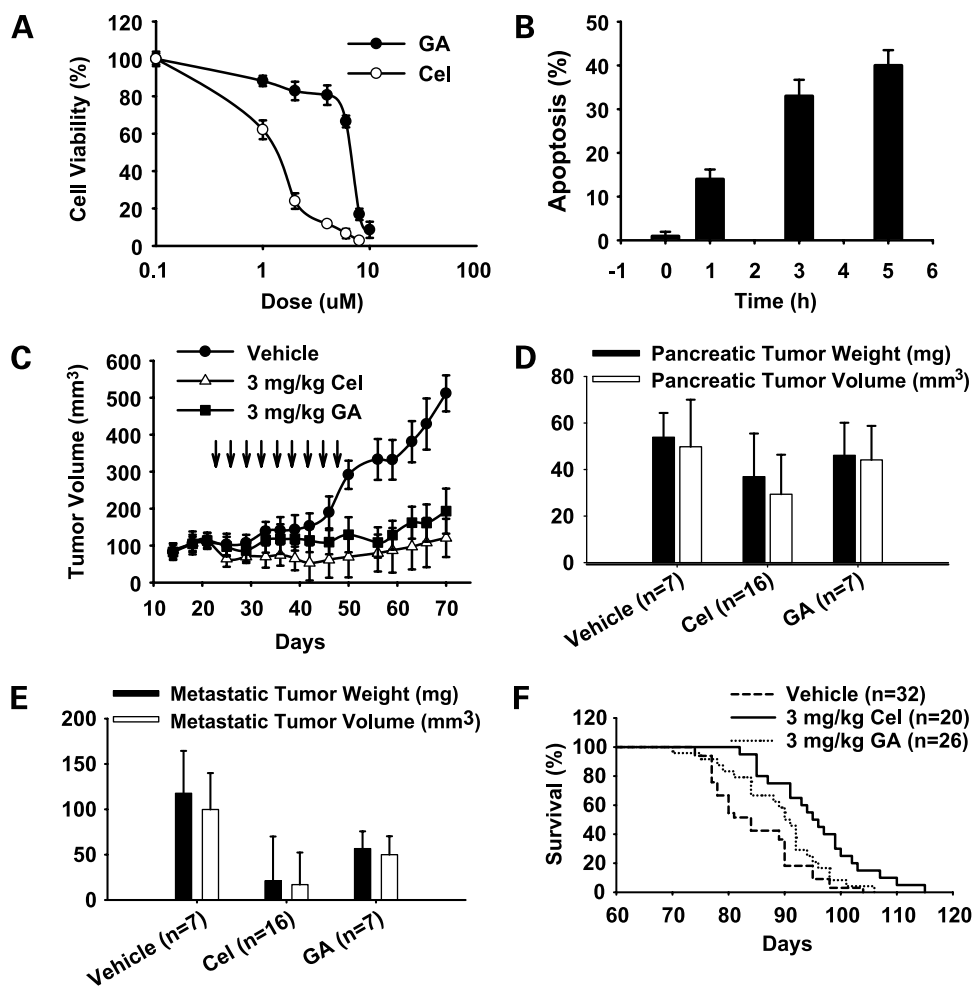
We further examined whether the mode of celastrol binding to the new binding site of Hsp90 could disrupt Hsp90-Cdc37 binding. Hsp90-celastrol complex was superimposed and replaced the Hsp90 protein in the Hsp90-Cdc37 crystal structure. This new complex was submitted to a long molecular dynamic simulation ( $\sim 4$  ns). The simulated (Hsp90-celastrol)-Cdc37 complex is depicted in

Fig. 1E. Celastrol was found in the mouth of the nucleotide-binding pocket. The three strongest H-bonds stabilizing celastrol in this orientation are still formed by the side chain of Arg<sup>32</sup>, Glu<sup>33</sup>, and Gly<sup>118</sup> residues. As mentioned above, celastrol filled the binding pocket by forming a  $\pi$ - $\pi$  stacking interaction with Arg<sup>32</sup>. The carboxylate of celastrol was involved in a network of H-bonds with the Arg<sup>32</sup> and His<sup>197</sup> side chains. The results showed that celastrol induced a major conformational change in the binding pocket, which disrupted an essential H-bond interaction between Arg<sup>167</sup> of Cdc37 and Glu<sup>33</sup> of Hsp90. This should significantly decrease the binding affinity of Cdc37 co-chaperone to its cognate Hsp90, thus disrupting the Hsp90-Cdc37 interaction.

In the Hsp90 superchaperone complex, the current understanding of the Hsp90-p23 interaction depicts p23 binding to the mature complex of Hsp90 (9). To predict whether celastrol prevents the interaction of Hsp90 and p23/Sba1 co-chaperone, we superimposed the Hsp90-celastrol complex with the X-ray structure of the Hsp90-p23 interaction (Fig. 1F). The results showed that the formation of the Hsp90-celastrol complex requires the lid segment residues being close to residues 26 to 33. The Hsp90 protein existed in two remarkably different conformations in the available X-ray crystal structures. In the structures reported for both the free Hsp90 protein and Hsp90-Cdc37 complex, the lid segment residues were close to residues 26 to 33. In the structure of the Hsp90-p23 complex, Hsp90 was in a different conformation in which the lid segment was completely displaced and was close to residues 36 to 50. Moreover, the aforementioned celastrol-binding pocket of Hsp90 is filled by residues 376 to 385 on



**Figure 4.** Effects of celastrol on client protein degradation and Hsp70 induction. **A**, celastrol and geldanamycin induces concentration-dependent decreases of Hsp90 client proteins measured by Western blot. **B**, celastrol causes time-dependent decrease of Hsp90 client proteins measured by Western blot. **C**, both celastrol and geldanamycin induce accumulation of Hsp70 protein measured by Western blot.



**Figure 5.** Antitumor effects of celastrol *in vitro* and *in vivo*. **A**, celastrol inhibits pancreatic cancer cell proliferation by MTS assay. **B**, celastrol (5  $\mu\text{mol/L}$ ) induces apoptosis by Annexin V staining. **C**, anti-tumor activity of celastrol against Panc-1 xenograft model. Arrows, dosing time. **D** to **F**, celastrol inhibits tumor growth in RIP1-Tag2 transgenic mouse model with pancreatic islet cell carcinoma. **D**, comparison of weights and volumes of the primary pancreatic islet cell carcinoma in each group when the RIP1-Tag2 mice were sacrificed at week 12. **E**, comparison of the metastatic tumor weights and volumes in each group when the RIP1-Tag2 mice were sacrificed at week 12. **F**, survival rate of the RIP1-Tag2 mice for each drug treatment group.

the Hsp90 COOH terminal in the Hsp90-p23 complex. The conformation of Hsp90 in the Hsp90-p23 complex is clearly not suitable for binding with celastrol. Hence, celastrol is not expected to disrupt the Hsp90-p23 complex.

#### Celastrol Has No Effect on ATP Binding to Hsp90

The molecular docking results showed that celastrol disrupted Hsp90-Cdc37 interaction without blocking the ATP-binding pocket of Hsp90. To further confirm this finding, we employed the ATP-Sepharose pull-down assay using purified human Hsp90 $\beta$  protein. As shown in Fig. 2A, ATP-Sepharose beads successfully pulled down Hsp90 in the solution. Geldanamycin has been reported to block the ATP-binding pocket of Hsp90. We also found that 1  $\mu\text{mol/L}$  geldanamycin was able to block more than 90% of Hsp90 $\beta$ -ATP binding. In contrast, celastrol (0.1-100  $\mu\text{mol/L}$ ) did not have an effect on ATP binding. This result provides further evidence that celastrol functioned differently from classic Hsp90 inhibitors (geldanamycin).

#### Celastrol Disrupts the Hsp90-Cdc37 Interaction in Pancreatic Cancer Cells

Hsp90 has interaction with various cochaperones at different stages of the catalytic cycle. Current studies have suggested that Hsp90, Cdc37, and Hop coexist in the

intermediate complex (20, 21). To confirm the molecular modeling results that celastrol disrupts the Hsp90-Cdc37 interaction, we did immunoblot analysis of Cdc37 and Hop after immunoprecipitation of Hsp90. As shown in Fig. 2B, immunoprecipitation of Hsp90 pulled down Cdc37 and Hop as detected by Western blot, which suggests that Hsp90-Cdc37 and Hsp90-Hop form a complex. Celastrol (10  $\mu\text{mol/L}$ ) decreased the amount of Cdc37 dramatically in the immunoprecipitated Hsp90 complex as early as 1 h after treatment; however, celastrol did not change the Hsp90-Hop interaction as indicated in the unchanged amount of Hop. In contrast, geldanamycin (10  $\mu\text{mol/L}$ ) did not change the level of either Hop or Cdc37 in immunoprecipitated Hsp90 complex. These results indicate that celastrol acts differently from geldanamycin by inhibiting Hsp90 through disruption of the Hsp90-Cdc37 complex. The unchanged levels of Hop and Cdc37 in the immunoprecipitated complex after geldanamycin treatment further confirmed that Cdc37 and Hop coexist in the intermediate Hsp90 superchaperone complex.

Unlike Cdc37, p23 is believed to be part of the mature superchaperone complex after ATP binding (17, 22, 23). To further confirm our molecular docking results that the

Hsp90-p23 complex could not accommodate celestrol binding, we did Western blot analysis for p23 after Hsp90 immunoprecipitation. Anti-Hsp90 antibody was able to pull down p23, indicating their interaction (Fig. 3A). Interestingly, after 24 h celestrol treatment, p23 was still present in the immunoprecipitated Hsp90 complex (Fig. 3A). The presence of Hsp90-p23 complex after celestrol treatment was further confirmed after immunoprecipitation of p23 (Fig. 3B), suggesting that celestrol does not disrupt the Hsp90-p23 complex in pancreatic cancer cells. As a comparison, because geldanamycin locks Hsp90 in the intermediate complex with Hop and Cdc37, Hsp90 is unlikely to bind p23 as the mature complex after geldanamycin treatment. Indeed, geldanamycin excluded p23 in the immunoprecipitated Hsp90 complex (Fig. 3A) and further excluded Hsp90 after immunoprecipitation of p23 (Fig. 3B). These data suggest that celestrol shows a different mechanism for Hsp90 inhibition compared with geldanamycin.

#### P23 Does Not Coexist with Cdc37 or Hop

Our data showed that celestrol and geldanamycin treatment led to distinct results, in which celestrol disrupted the Hsp90-Cdc37 interaction. Because geldanamycin has been reported to lock Hsp90 in the intermediate complex, which excludes Hsp90-p23 interaction, we intend to further elucidate the sequence of protein-protein interaction for Hsp90-Cdc37 and Hsp90-p23. We used antibodies against Cdc37, Hop, and Hsp90 to observe protein levels after p23 was immunoprecipitated. The results showed that Hsp90 was detected in the immunoprecipitated p23 complex, whereas neither Hop nor Cdc37 was detected (Fig. 3C). These results suggest that Cdc37 and Hop do not coexist with p23 in the Hsp90 super-chaperone complex. This further confirms that Cdc37 and Hop are in the intermediate complex of Hsp90, whereas p23 is in the mature complex. Our data are in

agreement with the recent crystal structure of Hsp90/Cdc37 and Hsp90/p23. The structural analysis has revealed that Cdc37 binds to the NH<sub>2</sub>-terminal binding domain of Hsp90 and arrests the chaperoning cycle in the conformation that could inhibit the binding of p23 to Hsp90 (14). Subsequently, *in vitro* difference circular dichroism suggests that binding of p23 and Cdc37 to Hsp90 is mutually exclusive (24).

#### Celestrol Decreases Hsp90 Client Protein Levels

Because celestrol resulted in the dissociation of Cdc37 from Hsp90, we next tested whether the compound could inhibit Hsp90 function and induce the degradation of its client proteins in pancreatic cells (Panc-1). Panc-1 cells were treated with various concentrations of celestrol or geldanamycin. The protein levels of Akt and Cdk4, two well-known Hsp90 clients (25, 26), were measured. Celestrol decreased the protein levels of Akt and Cdk4 in a time- and concentration-dependent manner. A 24-h treatment of Panc-1 cells with 1  $\mu$ mol/L celestrol slightly decreased Akt and Cdk4, but 5  $\mu$ mol/L celestrol was able to decrease Akt and Cdk4 by 80% and 70%, respectively (Fig. 4A and B). Similarly, geldanamycin induced similar levels of Akt and Cdk4 degradation (Fig. 4A). These data suggest that celestrol also induces Hsp90 client protein degradation although through a different mechanism.

In addition, geldanamycin usually does not change the levels of Hsp90 but induces Hsp70 protein expression. Western blot analysis confirmed that neither celestrol nor geldanamycin had any effect on Hsp90 protein levels. On the contrary, both celestrol (5  $\mu$ mol/L) and geldanamycin (5 and 10  $\mu$ mol/L) were able to increase Hsp70 protein expression by more than 12-fold after 24 h (Fig. 4C).

#### Celestrol Inhibits Panc-1 Cell Growth and Induces Apoptosis

Pancreatic cancer cells are usually resistant to various chemotherapeutic compounds. We selected the pancreatic

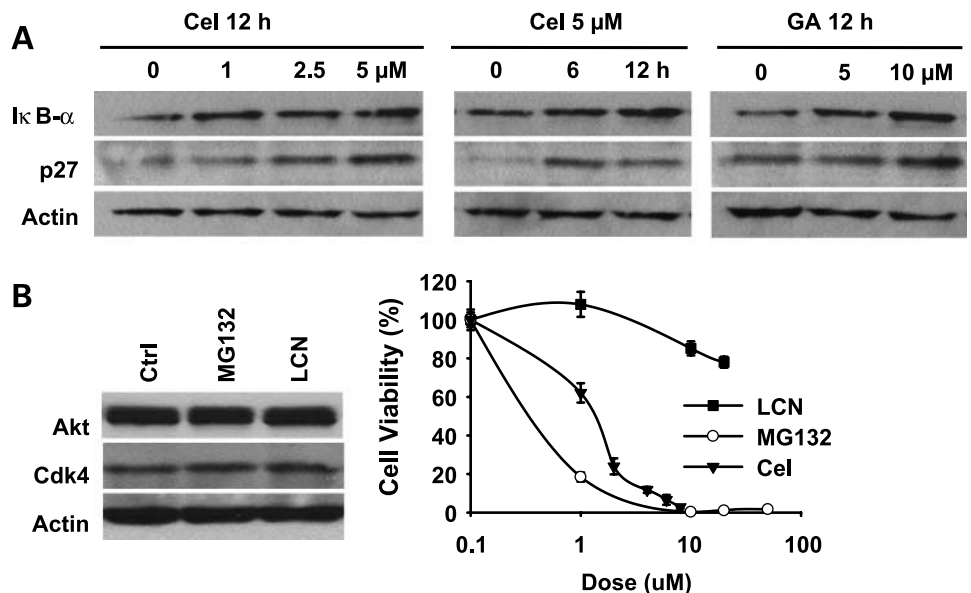


**Figure 6.** Celestrol is different from other proteasome inhibitors. **A**, both celestrol and geldanamycin (GA) induce the accumulation of p27 and I $\kappa$ B $\alpha$ . Panc-1 cells were treated with celestrol and geldanamycin. Protein levels of p27 and I $\kappa$ B $\alpha$  were analyzed by Western blot using specific antibodies. **B**, proteasome inhibitor MG132 and lactacystin (LCN) do not down-regulate Hsp90 client proteins. Panc-1 cells were treated with increasing concentrations of lactacystin or MG132 for 24 h. Cell viability was analyzed by MTS assay. Panc-1 cells were treated with 10  $\mu$ mol/L lactacystin or MG132 for 24 h. Protein levels of Akt and Cdk4 were analyzed by Western blot using specific antibodies.

cancer cell line (Panc-1) to test the anticancer effect of celastrol. MTS assay showed that celastrol exhibited stronger anticancer activity ( $IC_{50}$ , 3  $\mu\text{mol/L}$ ) than geldanamycin ( $IC_{50}$ , 8  $\mu\text{mol/L}$ ; Fig. 5A). Annexin V staining indicated that celastrol (5  $\mu\text{mol/L}$ ) induced apoptosis in ~15% to 40% of pancreatic cancer cells after 1 to 5 h of incubation (Fig. 5B). Pancreatic cancer cells became rounded and congregated after incubation with celastrol as early as 1 hour.

#### Celastrol Shows Strong Anticancer Activity *In vivo*

Because celastrol showed anticancer activity against pancreatic cancer cells *in vitro*, we then tested its activity *in vivo* with two models.

In Panc-1 cell xenograft mice, celastrol inhibited 80% of tumor growth ( $P < 0.001$ ) after the last injection (Fig. 5C). The anticancer effect of celastrol was slightly better than that of geldanamycin. Three weeks after the last injection, the average tumor size of the control group reached over 500  $\text{mm}^3$ , whereas the tumor size in celastrol treatment group was 4- to 5-fold smaller than the control group. It is worth noting that celastrol treatment caused 5% of weight loss in mice (data not shown).

We next used the RIP1-Tag2 transgenic mouse model of pancreatic islet carcinogenesis. Although pancreatic islet cell carcinomas are rare tumors with ~1 in 100,000 population, representing only 1% to 2% of all pancreatic neoplasms, they are quite resistant to standard therapy (27). The RIP1-Tag2 transgenic mice, which express multistage islet and metastatic tumors, provide an animal model for studying pancreatic endocrine tumors. In this model, hyperplastic islets begin to appear by 3 to 4 weeks of age, and solid tumors emerge in the pancreas at about 8 to 9 weeks. The tumors will metastasize into other sites, such as mesenterium, in the peritoneal cavity after 10 to 12 weeks. We found that celastrol decreased metastatic tumors in the mesenterium by 80% ( $P < 0.05$ ) and the tumors in the pancreas by 30% ( $P = 0.1$ ) compared with the control group after 4-week treatment (Fig. 5D and E). In comparison, geldanamycin inhibited metastatic tumors in the mesenterium by 50% ( $P < 0.05$ ) and tumors in the pancreas by 13% ( $P = 0.1$ ; Fig. 5D and E).

The RIP1-Tag2 transgenic mice generally have a lifespan of 11 to 13 weeks due to pancreatic tumor burden and related symptoms. Surprisingly, the inhibitory effect of celastrol on tumor growth led to a significant life prolongation. As shown in Fig. 5F, the median survival time for control and celastrol treatment group was 84 and 96 days, representing an average increase of 12 days ( $P < 0.001$ ). The geldanamycin treatment group only increased survival by 6 days ( $P < 0.001$ ). These data indicate that celastrol can inhibit the proliferation and metastasis of pancreatic islet carcinomas. Again, it is worth noting that celastrol resulted in a 10% weight loss for the mice (data not shown).

#### Celastrol Is Different from Other Proteasome Inhibitors

To test whether celastrol also inhibited the proteasome, we measured two well-known target proteins (p27 and  $I\kappa B\alpha$ ) of the proteasome in pancreatic cancer cells (28, 29).

The results showed that celastrol rendered the accumulation of cyclin-dependent kinase inhibitor p27 and  $I\kappa B\alpha$  (Fig. 6A). Interestingly, geldanamycin also showed a similar effect as celastrol for the protein levels of p27 and  $I\kappa B\alpha$  (Fig. 6A). To distinguish celastrol from other proteasome inhibitor, we next compared celastrol with proteasome inhibitors MG132 and lactacystin (30, 31) and observed their effect on Hsp90 client proteins (Akt and Cdk4). In contrast to celastrol, MG132 or lactacystin (10  $\mu\text{mol/L}$ ) did not change the levels of the Cdk4 and Akt proteins (Fig. 6B). MTS assay was used to show the antiproliferation effect (Fig. 6B). These results suggest that celastrol, which inhibits Hsp90-Cdc37 interaction, is distinct from other proteasome inhibitors.

#### Discussion

Targeted therapy appears to be an attractive approach for cancer therapy because it specifically targets malfunctioning proteins and signaling pathways (32). However, how to block multiple molecules and pathways remains a major challenge. The Hsp90 protein has emerged as a promising target with its regulation of many oncogenic proteins (9). In human pancreatic cancer, Hsp90 is expressed 6- to 7-fold higher than normal tissues (33). Recent data reveal that Hsp90 inhibitor (geldanamycin) has exhibited antitumor effect in nude mice implanted with human pancreatic cancer cells in combination with the glycolysis inhibitor.<sup>4</sup>

The Hsp90 protein is a weak ATPase and its function depends on the ability to bind and hydrolyze ATP (34). The early Hsp90 inhibitors represented by geldanamycin, herbimycin A and radicicol, target at the  $\text{NH}_2$ -terminal binding domain (35, 36). To date, many studies focused around these naturally occurring compounds, producing geldanamycin derivatives (such as 17-allylamino-geldanamycin; ref. 37), or synthesizing new compounds with similar binding capacity (e.g., CCT018159; ref. 38). Given that no Hsp90 inhibitor has reached the market place for cancer patients, it is premature to conclude that targeting the ATP-binding sites is a viable strategy for Hsp90 inhibition.

In the current study, we provided evidence for a novel Hsp90 inhibitor by disrupting protein-protein interaction in the Hsp90 superchaperone complex without blocking ATP binding. Celastrol disrupts the Hsp90/Cdc37 complex and leads to the degradation of Hsp90 client proteins. Celastrol exhibits antipancreatic tumor activity both *in vitro* and *in vivo*. This class of compound may offer a new strategy to develop novel Hsp90 inhibitors for treatment of pancreatic cancers.

The Hsp90 superchaperone complex has been studied extensively (10, 39). A client protein first binds to the Hsp70/Hsp40 complex and then Hop recruits the "open" state Hsp90 to the Hsp70-Hsp40-client complex. The binding of ATP to Hsp90 alters its conformation and

<sup>4</sup> Unpublished data.

results in the “closed” state. Hsp70, Hsp40, and Hop are subsequently released and replaced by another set of cochaperones, including p23 and immunophilins. With regard to the cochaperone Cdc37, the Hsp70/Hsp40 complex prepares the kinase for interaction with Cdc37 and then Cdc37 recruits Hsp90 to the complex (20, 21, 40). However, on ATP binding, whether Cdc37 dissociates or p23 binds has remained unclear. Our data of p23 immunoprecipitation suggest that p23 does not coexist with either Cdc37 or Hop (Fig. 3C). The recent structural study of Hsp90/Cdc37 has shown that Cdc37 binds to the NH<sub>2</sub>-terminal domain of Hsp90 by inserting its COOH-terminal side chain into the nucleotide-binding pocket, holding Hsp90 in an “open” conformation (14). Therefore, progression from this stage through the ATPase cycle requires the ejection of Cdc37 side chain from the binding pocket (14). *In vitro* protein binding analysis also suggests that binding of Cdc37 and p23 to Hsp90 is mutually exclusive and the p23-Hsp90-Cdc37 complex could not exist (24). Taken together, the data imply that Cdc37 dissociates from the Hsp90 superchaperone complex after ATP binding. Moreover, Cdc37 and p23 bind at different stages of the chaperoning cycle.

Geldanamycin locks Hsp90 in the intermediate complex of the client protein loading phase (9). Therefore, geldanamycin effectively halts the chaperoning cycle and leads to proteasomal degradation of client protein (9, 10). Consistent with these findings, our data showed that geldanamycin inhibited the binding of ATP to Hsp90 (Fig. 2A). Incubating pancreatic cancer cells with geldanamycin led to degradation of Hsp90 client proteins (Akt and Cdk4; Fig. 4A). Because geldanamycin locks Hsp90 in the intermediate complex, Hsp90 is unlikely to proceed to the subsequent states of binding p23 (17, 22, 23). Therefore, the Hsp90-p23 complex was not detected in Panc-1 cells after geldanamycin treatment (Fig. 3A and B), which is also consistent with previous studies that p23 only binds to ATP-bound form of Hsp90. However, the Hsp90-Cdc37 or Hsp90-Hop complex showed no difference after geldanamycin treatment (Fig. 2B), indicating that Hsp90-Cdc37 or Hsp90-Hop coexists in the intermediate complex, which could be arrested by geldanamycin.

In contrast to geldanamycin, celastrol provides a distinct mechanism for Hsp90 inhibition. Our computational modeling and coimmunoprecipitation data confirmed that celastrol interfered with the Hsp90-Cdc37 interaction (Figs. 1E and 2B). As a consequence, Hsp90 clients were degraded in the time- and dose-dependent manner (Fig. 4A and B). However, celastrol did not interrupt the Hsp90-p23 complex in pancreatic cancer cells (Fig. 3A and B), although different results have been reported in SKBR-3 cells (13). The computer modeling also showed p23 blocked the access of celastrol to its binding site in the Hsp90/p23 complex (Fig. 1F). Our data and previous studies may explain the sequence of chaperoning cycles in Hsp90 superchaperone complex. The previous results have shown that the COOH terminus of Cdc37 inserts into the ATP-binding pocket of Hsp90 (open state), later ATP binding to Hsp90 ejects Cdc37

from Hsp90 (14), setting up the stage for binding of p23 to Hsp90. Therefore, Cdc37 and p23 bind to Hsp90 at different stages of the chaperoning cycle without coexisting in one complex. Rather, Cdc37 ejection from Hsp90 seems to be the prerequisite for p23 binding. Therefore, disruption of the Hsp90-Cdc37 complex by celastrol may not affect the Hsp90-p23 complex. In contrast, it may help to eject Cdc37 from Hsp90 and prepare Hsp90 to bind to p23.

Recent studies have extended the investigation of Hsp90 inhibition from its direct effect on cancer cells to the cellular functions required for tumor invasion and metastasis. Several protein kinases promoting cancer cell invasion and metastasis have been reported to be Hsp90 clients, and their expression and activity are affected by Hsp90 inhibitors (41). It has also been shown that Hsp90 inhibitor geldanamycin suppresses extrinsic stimuli-induced signaling pathways contributing to tumor invasion and angiogenesis in T24 bladder carcinoma model (42). Consistent with those findings, the dosing of celastrol or geldanamycin to the RIP1-Tag2 transgenic mice has dramatically reduced the metastatic tumor sizes by 80% and 30%, much more than the reduction in primary pancreatic islet carcinomas, which were 30% and 13%, respectively (Fig. 5D and E). Varying levels of dependence on Hsp90 may account for the differential effect of Hsp90 inhibition during progression of primary and metastatic tumors. However, further studies are required to clarify the role of Hsp90 in tumor metastasis.

It has been reported that celastrol is a proteasome inhibitor by Yang et al. (18). Consistent with their results, we also confirmed that celastrol induced the accumulation of proteasomal target proteins p27 and I $\kappa$ B $\alpha$  in Panc-1 cells (Fig. 6A). Interestingly, the classic Hsp90 inhibitor geldanamycin also induced the accumulation of p27 and I $\kappa$ B $\alpha$  (Fig. 6A). Furthermore, celastrol differed from other proteasome inhibitors (MG132 and lactacystin) by causing degradation of Hsp90 client proteins, whereas MG132 or lactacystin had no effect (Fig. 6B). These data suggest that celastrol is different from the classic proteasomal inhibitor for its anticancer activity.

In conclusion, celastrol exhibited potent anticancer activity against pancreatic cancer cells (Panc-1) *in vitro* and *in vivo* in xenografts. Celastrol also inhibited the tumor metastasis in the RIP1-Tag2 transgenic mice model of pancreatic islet carcinomas. Computer modeling and immunoprecipitation confirmed that celastrol disrupted the protein-protein interaction of Hsp90-Cdc37, resulting in the induction of Hsp90 client protein degradation. In contrast to the classic Hsp90 inhibitor geldanamycin, celastrol did not interfere with the ATP binding to Hsp90. These data suggest that celastrol disrupts Hsp90-Cdc37 interaction and provides a novel mechanism for Hsp90 inhibition against pancreatic cancer cells.

#### Acknowledgments

We thank Dr. David Toft for the generous gifts of the purified Hsp90 $\beta$  protein and H9010 antibody to Hsp90 and the Center for Computational Sciences at University of Kentucky for support in supercomputing time.



**References**

1. Jemal A, Siegel R, Ward E, Murray T, Xu J, Thun MJ. Cancer statistics, 2007. *CA Cancer J Clin* 2007;57:43–66.
2. Evans DB, Abbruzzese JL, Rich TR. Cancer of the pancreas. In: De Vita VT, Hellman S, Rosenberg SA, editors. *Cancer principles and practice of oncology* 5th ed. Philadelphia: JB Lippincott; 1997. p. 1054–87.
3. Sawyers C. Targeted cancer therapy. *Nature* 2004;432:294–7.
4. Iwata H. Perspective of trastuzumab treatment. *Breast Cancer* 2007;14:150–5.
5. Kindler HL, Friberg G, Singh DA, et al. Phase II trial of bevacizumab plus gemcitabine in patients with advanced pancreatic cancer. *J Clin Oncol* 2005;23:8033–40.
6. Xiong HQ, Rosenberg A, LoBuglio A, et al. Cetuximab, a monoclonal antibody targeting the epidermal growth factor receptor, in combination with gemcitabine for advanced pancreatic cancer: a multicenter phase II trial. *J Clin Oncol* 2004;22:2610–6.
7. Safran H, Iannitti D, Ramanathan R, et al. Herceptin and gemcitabine for metastatic pancreatic cancers that overexpress HER-2/*neu*. *Cancer Invest* 2004;22:706–12.
8. Neckers L. Hsp90 inhibitors as novel cancer chemotherapeutic agents. *Trends Mol Med* 2002;8:55–61.
9. Kamal A, Boehm MF, Burrows FJ. Therapeutic and diagnostic implications of Hsp90 activation. *Trends Mol Med* 2004;10:283–90.
10. Neckers L. Development of small molecule Hsp90 inhibitors: utilizing both forward and reverse chemical genomics for drug identification. *Curr Med Chem* 2003;10:733–9.
11. Ramanathan RK, Trump DL, Eiseman JL, et al. Phase I pharmacokinetic-pharmacodynamic study of 17-(allylamino)-17-demethoxyGA (17AAG, NSC 330507), a novel inhibitor of heat shock protein 90, in patients with refractory advanced cancers. *Clin Cancer Res* 2005;11:3385–91.
12. Westerheide SD, Bosman JD, Mbadugha BN, et al. Celastrols as inducers of the heat shock response and cytoprotection. *J Biol Chem* 2004;279:56053–60.
13. Hieronymus H, Lamb J, Ross KN, et al. Gene expression signature-based chemical prediction identifies a novel class of HSP90 pathway modulators. *Cancer Cell* 2006;10:321–30.
14. Roe SM, Ali MMU, Meyer P, et al. The mechanism of Hsp90 regulation by the protein kinase-specific cochaperone p50(cdc37). *Cell* 2004;116:87–98.
15. Bernstein FC, Koetzle TF, Williams GJ, et al. The Protein Data Bank: a computer-based archival file for macromolecular structures. *J Mol Biol* 1977;112:535–42.
16. Ali MM, Roe SM, Vaughan CK, et al. Crystal structure of an Hsp90-nucleotide-p23/Sba1 closed chaperone complex. *Nature* 2006;440:1013–7.
17. Grenert JP, Sullivan WP, Fadden P, et al. The amino-terminal domain of heat shock protein 90 (hsp90) that binds GA is an ATP/ADP switch domain that regulates hsp90 conformation. *J Biol Chem* 1997;272:23843–50.
18. Yang H, Chen D, Cui QC, Yuan X, Dou QP. Celastrol, a triterpene extracted from the Chinese “Thunder of God Vine,” is a potent proteasome inhibitor and suppresses human prostate cancer growth in nude mice. *Cancer Res* 2006;66:4758–65.
19. Hamza A, Zhan CG. How can (-)-epigallocatechin gallate from green tea prevent HIV-1 infection? Mechanistic insights from computational modeling and the implication for rational design of anti-HIV-1 entry inhibitors. *J Phys Chem B Condens Matter Mater Surf Interfaces Biophys* 2006;110:2910–7.
20. Lee P, Shabbir A, Cardozo C, Caplan AJ. St1 and Cdc37 can stabilize Hsp90 in chaperone complexes with a protein kinase. *Mol Biol Cell* 2004;15:1785–92.
21. Pearl LH. Hsp90 and Cdc37—a chaperone cancer conspiracy. *Curr Opin Genet Dev* 2005;15:55–61.
22. Johnson JL, Toft DO. Binding of p23 and hsp90 during the assembly with the progesterone receptor. *Mol Endocrinol* 1995;9:670–8.
23. Sullivan W, Stensgard B, Caucutt G, et al. Nucleotides and two functional states of hsp90. *J Biol Chem* 1997;272:8007–12.
24. Siligardi G, Hu B, Panaretou B, Piper PW, Pearl LH, Prodromou C. Cochaperone regulation of conformational switching in the Hsp90 ATPase cycle. *J Biol Chem* 2004;279:51989–98.
25. Sato S, Fujita N, Tsuruo T. Modulation of Akt kinase activity by binding to Hsp90. *Proc Natl Acad Sci U S A* 2000;97:10832–7.
26. Stepanova L, Leng XH, Parker SB, Harper JW. Mammalian p50(Cdc37) is a protein kinase-targeting subunit of Hsp90 that binds and stabilizes Cdk4. *Genes Dev* 1996;10:1491–502.
27. Oberg K, Eriksson B. Endocrine tumours of the pancreas. *Best Pract Res Clin Gastroenterol* 2005;19:753–81.
28. Schulte TW, An WG, Neckers LM. GA-induced destabilization of Raf-1 involves the proteasome. *Biochem Biophys Res Commun* 1997;239:655–9.
29. Verma IM, Stevenson JK, Schwarz EM, Van Antwerp D, Miyamoto S. Rel/NF- $\kappa$ B/I $\kappa$ B family: intimate tales of association and dissociation. *Genes Dev* 1995;9:2723–35.
30. Kisselev AF, Goldberg AL. Proteasome inhibitors: from research tools to drug candidates. *Chem Biol* 2001;8:739–58.
31. Fenteany G, Standaert RF, Lane WS, Choi S, Corey EJ, Schreiber SL. Inhibition of proteasome activities and subunit-specific amino-terminal threonine modification by lactacystin. *Science* 1995;268:726–31.
32. Xiong HQ. Molecular targeting therapy for pancreatic cancer. *Cancer Chemother Pharmacol* 2004;54 Suppl 1:S69–77.
33. Ogata M, Naito Z, Tanaka S, Moriyama Y, Asano G. Overexpression and localization of heat shock proteins mRNA in pancreatic carcinoma. *J Nippon Med Sch* 2000;67:177–85.
34. Prodromou C, Roe SM, O’Brien R, Ladbury JE, Piper PW, Pearl LH. Identification and structural characterization of the ATP/ADP-binding site in the Hsp90 molecular chaperone. *Cell* 1997;90:65–75.
35. Whitesell L, Mimnaugh EG, De Costa B, Myers CE, Neckers LM. Inhibition of heat shock protein HSP90-60v-src heteroprotein complex formation by benzoquinone ansamycins: essential role for stress proteins in oncogenic transformation. *Proc Natl Acad Sci U S A* 1994;91:8324–8.
36. Schulte TW, Akinaga S, Soga S, et al. Antibiotic radicicol binds to the N-terminal domain of Hsp90 and shares important biologic activities with GA. *Cell Stress Chaperones* 1998;3:100–8.
37. Schulte TW, Neckers LM. The benzoquinone ansamycin 17-allylamino-17-demethoxyGA binds to HSP90 and shares important biologic activities with GA. *Cancer Chemother Pharmacol* 1998;42:273–9.
38. Dymock BW, Barril X, Brough PA, et al. Novel, potent small-molecule inhibitors of the molecular chaperone Hsp90 discovered through structure-based design. *J Med Chem* 2005;48:4212–5.
39. Richter K, Buchner J. Hsp90: chaperoning signal transduction. *J Cell Physiol* 2001;188:281–90.
40. Arlander SJ, Felts SJ, Wagner JM, Stensgard B, Toft DO, Karnitz LM. Chaperoning checkpoint kinase 1 (Chk1), an Hsp90 client, with purified chaperones. *J Biol Chem* 2006;281:2989–98.
41. Xu W, Neckers L. Targeting the molecular chaperone heat shock protein 90 provides a multifaceted effect on diverse cell signaling pathways of cancer cells. *Clin Cancer Res* 2007;13:1625–9.
42. Koga F, Tsutsumi S, Neckers LM. Low dose GA inhibits hepatocyte growth factor and hypoxia-stimulated invasion of cancer cells. *Cell Cycle* 2007;6:1393–402.